Phytochemistry 187 (2021) 112759

Contents lists available at ScienceDirect

Phytochemistry

journal homepage: www.elsevier.com/locate/phytochem

Cytotoxic triterpenoids from *Chisocheton pentandrus*

Supriatno Salam [a,c], Desi Harneti [a], Rani Maharani [a,b], Nurlelasari [a], Agus Safari [a], Ace Tatang Hidayat [a,b], Ronny Lesmana [b,d], Mohamad Azlan Nafiah [e], Unang Supratman [a,b,*], Thomas Alexander Kyle Prescott [f], Yoshihito Shiono [g]

[a] Department of Chemistry, Faculty of Mathematics and Natural Sciences, Universitas Padjadjaran, Jatinangor, 45363, Indonesia
[b] Central Laboratory, Universitas Padjadjaran, Jatinangor, 45363, Indonesia
[c] Faculty of Pharmacy, Universitas Mulawarman, Samarinda, 75123, Kalimantan Timur, Indonesia
[d] Physiology Division, Department of Biomedical Sciences, Faculty of Medicine, Universitas Padjadjaran, Jatinangor, 45363, Indonesia
[e] Department of Chemistry, Faculty of Science and Mathematics, Sultan Idris Education University, Tg Malim, 35900, Perak, Malaysia
[f] Royal Botanic Gardens, Kew, Richmond, Surrey TW9 3AB, United Kingdom
[g] Department of Food, Life, and Environmental Science, Faculty of Agriculture, Yamagata University, Tsuruoka, Yamagata, 997-8555, Japan

ARTICLE INFO

Keywords:
Chisocheton pentandrus
Meliaceae
Pentandrucine A-K
Cytotoxic activity
MCF-7
Triterpenoid

ABSTRACT

Eleven undescribed triterpenoids (pentandrucines A to K) were isolated from the *n*-hexane extract of the stem bark of *Chisocheton pentandrus* (Blanco) Merr. These comprised ten undescribed dammarane-type triterpenoids and one undescribed apotirucallane-type triterpenoid. Additionally, two dammarane-type triterpenoids, four apotirucallane-type triterpenoids and two tirucallane-type triterpenoids were also isolated. The chemical structures of pentandrucine A-K, were fully elucidated using 1D and 2D-NMR, and high resolution MS. All of the compounds were evaluated for cytotoxic activity against MCF-7 breast cancer cells *in vitro*. Melianodiol proved to be the most active with an IC_{50} of 16.84 μM comparing favourably with Cisplatin (13.2 μM).

1. Introduction

The genus *Chisocheton* belong to Meliaceae family comprises 150 species which are widely distributed throughout the tropics (Shilpi et al., 2016). Previous investigations have shown the diverse range of biologically active metabolites isolated from this genus, including cytotoxic limonoids (Awang et al., 2007; Maneerat et al., 2008; Yang et al., 2009; Nagoor et al., 2011; Nurlelasari et al., 2017; Supriatno et al., 2018; Supratman et al., 2020), cytotoxic triterpenoids (Wong et al., 2011; Huang et al., 2016; Katja et al., 2017; Supratman et al., 2019), and antimycobacterial sesquiterpenoids (Phongmaykin et al., 2008), as well as anti-inflammatory limonoids (Yang et al., 2011), the antifungal compound meliacin (Bordoloi et al., 1993), antimalarial limonoids (Maneerat et al., 2008), antimycobacterial limonoids (Maneerat et al., 2008; Phongmaykin et al., 2008) and antiplasmodial triterpenoids (Mohamad et al., 2009). In a previous paper, we confirmed the cytotoxicity of limonoids obtained from the stem bark of *Chisocheton pentandrus* (Blanco) Merr. against MCF-7 breast cancer line (Supriatno et al., 2018; Supratman et al., 2020). As a continuation, in the present paper we provide structural elucidation of eleven undescribed triterpenoids, including pentandrucine A-K (**1**–**11**) and eight triterpenoids. All compounds were evaluated for cytotoxic activity against MCF-7 breast cancer line.

2. Results and discussion

The methanol extract of *C. pentandrus* stem bark was dissolved in water and extracted successively with *n*-hexane, EtOAc and *n*-butanol. The *n*-hexane portion was fractionated using silica gel column chromatography (CC), leading to the isolation of eleven undescribed triterpenoids, pentandrucines (**1**–**11**), and eight triterpenoids (**12**–**19**) (Fig. 1).

The eight triterpenoid compounds were identified as cabrealeolactone (**12**) (Nagaya et al., 1997), cabraleadiol (**13**) (Phongmaykin et al., 2008), prototiamin A (**14**) (Happi et al., 2015), neemfruitin A (**15**) (Chianese et al., 2010), desmethyllimocin B (**16**) (Kumar et al., 1996), protoxylocarpin G (**17**) (Brahmachari et al., 2004), melianodiol (**18**) (Puripattanavong et al., 2000; Kurimoto et al., 2014) and indicalilacol B (**19**) (Kurimoto et al., 2014) by comparing the respective spectroscopic evidence with existing publications.

* Corresponding author. Department of Chemistry, Faculty of Mathematics and Natural Sciences, Universitas Padjadjaran, Jatinangor, 45363, Indonesia.
E-mail address: unang.supratman@unpad.ac.id (U. Supratman).

https://doi.org/10.1016/j.phytochem.2021.112759
Received 12 October 2020; Received in revised form 13 March 2021; Accepted 26 March 2021

Compound (**1**) was isolated as colorless needle crystals (MeOH), and is characterized by the molecular composition, $C_{29}H_{44}O_5$, based on HR-TOFMS (Fig. S1). This showed a $[M+H]^+$ ion peak at *m/z* 473.3271 (calcd. $C_{29}H_{45}O_5$ *m/z* 473.3241), hence eight degrees of unsaturation is required. In addition, the IR absorption bands at 2964, 2923, 1704 and 1085 cm^{-1} implied the presence of aliphatic, carbonyl and ether groups, while the ^1H NMR data displayed in Table 1 and Fig. S2, shows seven tertiary methyls at δ_H 0.81 (CH_3-29), 0.82 (CH_3-19), 0.87 (CH_3-30), 0.91 (CH_3-28), 0.92 (CH_3-18), 1.33 (CH_3-21) and 1.94 (CH_3-2′). Also, an oxygenated methine was identified at δ_H 5.21 (1H, br.s). Meanwhile, the ^{13}C NMR and DEPT spectrum data of **1** (Table 1, Fig. S3 and Fig. S4), where 29 nonequivalent carbons were distinguished, including seven tertiary methyls, nine sp^3 methylenes, five sp^3 methynes (comprising an oxygenated methyne at δ_C 76.3), five sp^3 quaternary carbons (including an oxygenated carbon at δ_C 90.3) and three carbonyls (comprising, ketones, lactone, and acetyl at δ_C 218.2, 176.9 and 170.1, respectively). These functionalities account for three out of eight degrees of unsaturation, therefore **1** requires the presence of five additional rings. Furthermore, the data provided above, alongside biogenetic considerations suggest **1** to be a dammarane-type triterpenoid, consisting of an acetyl group and a lactone ring (Nagaya et al., 1997; Bai et al., 2018). The NMR data was compared with 17α-hydroxycabralealactone isolated from the whole *Cleome africana* plant (Nagaya et al., 1997), and the structures appeared to be closely related. However, the main difference was observed in the absence of a hydroxyl group at C-7 and the presence of an acetyl at C-7 in **1**. In addition, the compound structure was deduced from the ^1H–^1H COSY and HMBC spectrum (Fig. 2a, Fig. S6 and Fig. S7), which attributes the assignment of seven singlet methyls to the possible correlations between tertiary methyl protons and neighboring carbons. This property is characteristic of a dammarane-type triterpenoid (Nagaya et al., 1997; Bai et al., 2018). Also, the correlation from oxygenated protons at H-7 (δ_H 5.21) to C-5 (δ_C 55.4), C-6 (δ_C 18.3), C-9 (δ_C 50.4) and C-1′ (δ_C 170.1), as well as methyl protons at CH_3-2′ (δ_H 1.94) to C-1′ (δ_C 170.1) were applied in the designation of an acetyl group at C-7. Proton at H-17 (δ_H 1.23) to C-20 (δ_C 90.3), C-21 (δ_C 25.4) and C-22 (δ_C 31.3), while proton CH_3-21 (δ_H 1.33) to C-17 (δ_C 49.5) and C-22 (δ_C 31.3) are the δ-lactone ring correlations.

The relative configuration of **1** was determined by NOESY (Fig. 2b and Fig. S8), which is supported by the presence of dammarane-type triterpenoids in *Chisocheton* species (Phongmaykin et al., 2008; Bai et al., 2018). The NOESY correlations H-7/CH_3-18 and CH_3-19 identified the acetyl group at C-7 as α-oriented, while the cross peak observed between CH_3-30/H-17/CH_3-21, indicates the δ-lactone ring present at C-17 and CH_3-21 as α-oriented. Differences between isocabralealactone and cabralealactone were located at the stereochemistry at C-20. The chemical shift of the proton and carbon from 20*S*-epimer (δ_H 1.39, δ_C 25.4) more downfield than those of 20*R*-epimer (δ_H 1.34, δ_C 22.08) (Joycharat et al., 2010; Gupta and Dev. 1971; Cascon and Brown, 1972; Ahmad and Alvi, 1987; Nagaya et al., 1997; Crabbe et al., 1958; Yamashita et al., 1998). Consequently, the structure of **1** was elucidated as a 7α-acetyl derivative of 17α-hydroxycabralealactone and termed pentandrucine A.

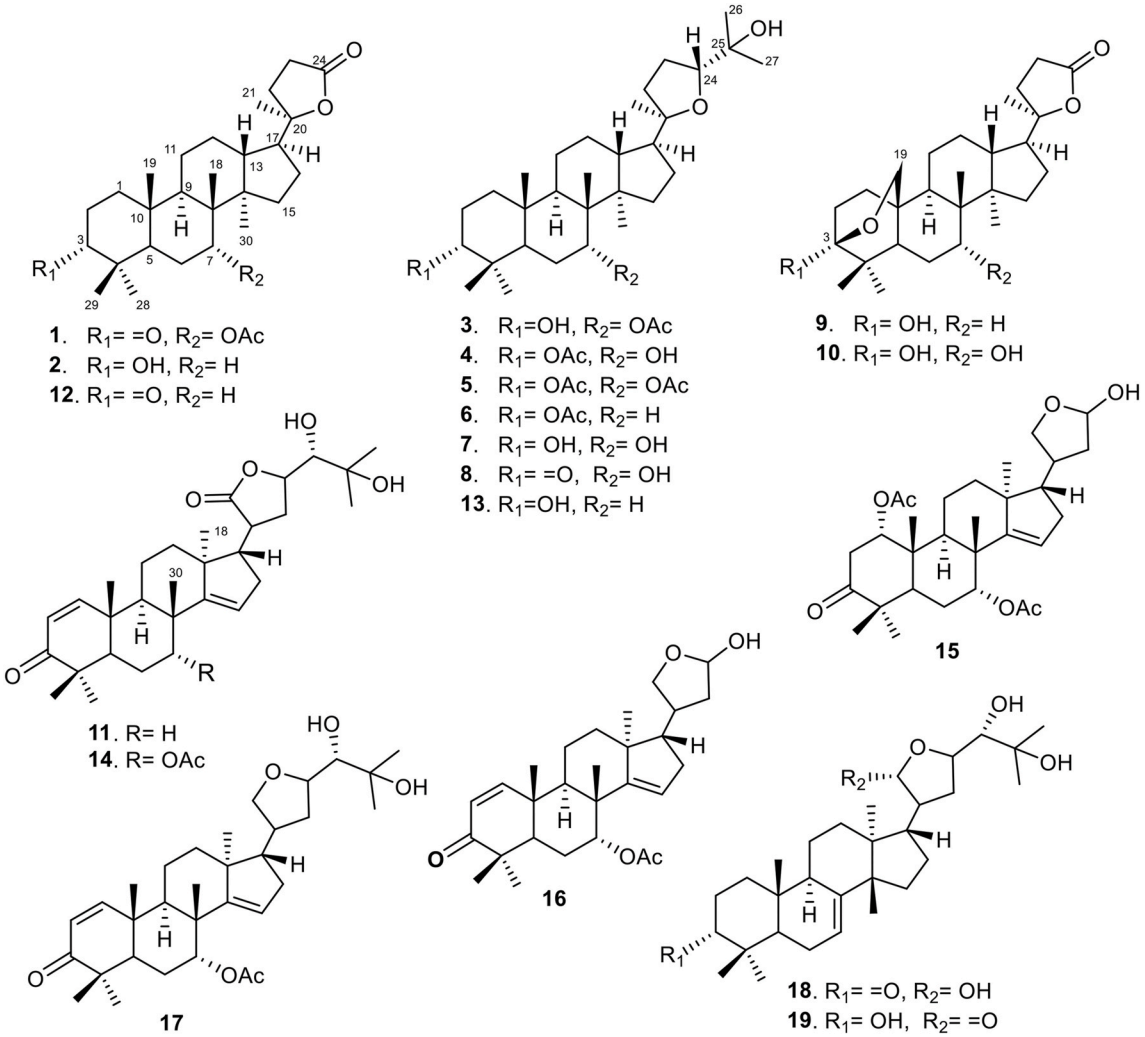

Fig. 1. Structures of Compounds **1**–**19**.

Table 1
NMR data for compounds **1–4** (500 MHz for ^{1}H and 125 MHz for ^{13}C in $CDCl_3$).

Position Carbon	1		2		3		4	
	^{13}C-NMR δ_C (mult.)	^{1}H-NMR δ_H [(ΣH, mult., *J*(Hz)]	^{13}C-NMR δ_C (mult.)	^{1}H-NMR δ_H [(ΣH, mult., *J*(Hz)]	^{13}C-NMR δ_C (mult)	^{1}H-NMR δ_H [(ΣH, mult, *J*(Hz)]	^{13}C-NMR δ_C (mult.)	^{1}H-NMR δ_H [(ΣH, mult, *J*(Hz)]
1	35.2 (t)	1.17 (1H, m) 1.50 (1H, m)	34.8 (t)	1.15 (1H, m) 1.50 (1H, m)	33.7 (t)	1.18 (1H, m) 1.54 (1H, m)	33.7 (t)	1.42 (1H, m) 1.62 (1H, m)
2	33.7 (t)	1.40 (1H. dd, 2.4, 9.6) 2.32 (1H, m)	33.7 (t)	1.45 (1H, dt, 2.4, 3.2) 2.74 (1H, m)	25.4 (t)	1.55 (1H, dd, 2.6, 9.8) 2.34 (1H, m)	25.4 (t)	1.55 (1H, dd, 2.5, 9.6) 2.35 (1H, m)
3	218.2 (s)	–	75.3 (d)	4.42 (1H, t, 3.2)	71.3 (d)	4.33 (1H, t, 3.0)	75.4 (d)	5.23 (1H, t, 3.0)
4	37.3 (s)	–	37.3 (s)	–	37.3 (s)	–	37.3 (s)	–
5	55.4 (d)	1.95 (1H, m)	55.4 (d)	1.85 (1H, m)	49.6 (d)	1.24 (1H, m)	49.6 (d)	1.24 (1H, m)
6	18.3 (t)	1.37 (1H, m) 2.07 (1H, m)	18.4 (t)	1.36 (1H, m) 2.05 (1H, m)	18.3 (t)	1.39 (1H, m) 2.06 (1H, m)	18.3 (t)	1.39 (1H, m) 2.07 (1H, m)
7	76.3 (d)	5.21 (1H, br.s)	34.7 (t)	1.39 (1H, m) 1.56 (1H, m)	75.4 (d)	5.23 (1H, br.s) –	71.3 (d)	3.43 (1H, t, 2.3)
8	40.6 (s)	–	40.6 (s)	–	40.7 (s)	–	40.7 (s)	–
9	50.4 (d)	1.41 (1H, dd, 2.4, 13.2)	50.4 (d)	1.41 (1H, dd, 2.4, 13.2)	50.7 (d)	1.44 (1H, m)	50.7 (d)	1.44 (1H, m)
10	37.7 (s)	–	37.7 (s)	–	37.7 (s)	–	37.7 (s)	–
11	25.4 (t)	1.20 (1H, m) 1.60 (1H, m)	25.4 (t)	1.20 (1H, m) 1.57 (1H, m)	21.7 (t)	1.53 (1H, m) 1.24 (1H, m)	21.7 (t)	1.53 (1H, m) 1.26 (1H, m)
12	21.3 (t)	1.49 (1H, m) 1.91 (1H, m)	21.3 (t)	1.49 (1H, m) 1.91 (1H, m)	27.1 (t)	1.75 (1H, m) 1.50 (1H, m)	27.1 (t)	1.75 (1H, m) 1.40 (1H, m)
13	43.2 (d)	1.53 (1H, m)	43.2 (d)	1.53 (1H, m)	42.8 (d)	1.62 (1H, m)	42.8 (d)	1.62 (1H, m)
14	50.3 (s)	–	50.3 (s)	–	50.2 (s)	–	50.2 (s)	–
15	31.2 (t)	1.90 (1H, m) 1.10 (1H, m)	31.2 (t)	1.90 (1H, m) 1.10 (1H, m)	31.5 (t)	1.04 (1H, m) 1.74 (1H, m)	31.5 (t)	1.04 (1H, m) 1.65 (1H, m)
16	25.1 (t)	1.52 (1H, m) 1.97 (1H, m)	25.1 (t)	1.52 (1H, m) 1.96 (1H, m)	25.9 (t)	1.51 (1H, m) 1.88 (1H, m)	25.9 (t)	1.51 (1H, m) 1.91 (1H, m)
17	49.5 (d)	1.23 (1H, m)	49.5 (d)	1.23 (1H, m)	49.8 (d)	1.83 (1H, m)	49.8 (d)	1.83 (1H, m)
18	15.6 (q)	0.92 (3H, s)	15.6 (q)	0.92 (3H, s)	16.2 (q)	0.95 (3H, s)	16.2 (q)	0.95 (3H, s)
19	16.1 (q)	0.82 (3H, s)	16.1 (q)	0.82 (3H, s)	16.6 (q)	0.84 (3H, s)	16.6 (q)	0.84 (3H, s)
20	90.3 (s)	–	90.4 (s)	–	86.7 (s)	–	86.7 (s)	–
21	25.4 (q)	1.33 (3H, s)	25.4 (q)	1.33 (3H, s)	27.3 (q)	1.13 (3H, s)	27.3 (q)	1.13 (3H, s)
22	31.3 (t)	1.47 (1H, m) 2.01 (1H, m)	31.3 (t)	1.47 (1H, m) 2.01 (1H, m)	35.3 (t)	1.22 (1H, m) 2.32 (1H, m)	35.3 (t)	1.22 (1H, m) 2.34 (1H, m)
23	29.3 (t)	2.52 (1H, d, 10) 2.62 (1H, d, 10)	29.3 (t)	2.52 (1H, d, 9.9) 2.62 (1H, d, 9.9)	26.4 (t)	1.85 (1H, m) 2.24 (1H, m)	26.4 (t)	1.85 (1H, m) 2.35 (1H, m)
24	176.9 (s)	–	176.7 (s)	–	86.3 (d)	3.62 (1H, dd, 4.8, 10.2)	86.3 (d)	3.62 (1H, dd, 4.8, 10.2)
25	–	–	–	–	70.3 (s)	–	70.3 (s)	–
26	–	–	–	–	27.9 (q)	1.17 (3H, s)	27.9 (q)	1.17 (3H, s)
27	–	–	–	–	24.1 (q)	1.09 (3H, s)	24.1 (q)	1.09 (3H, s)
28	28.4 (q)	0.91 (3H, s)	28.4 (q)	0.91 (3H, s)	28.4 (q)	0.92 (3H, s)	28.4 (q)	0.92 (3H, s)
29	22.2 (q)	0.81 (3H, s)	22.2 (q)	0.78 (3H, s)	22.2 (q)	0.82 (3H, s)	22.2 (q)	0.82 (3H, s)
30	16.4 (q)	0.87 (3H, s)	16.4 (q)	0.88 (3H, s)	15.6 (q)	0.87 (3H, s)	15.6 (q)	0.87 (3H, s)
1′	170.1 (s)	–	–	–	170.2 (s)	–	170.0 (s)	–
2′	21.2 (q)	1.94 (3H, s)	–	–	21.2 (q)	1.95 (3H, s)	21.1 (q)	1.91 (3H, s)

Compound **2** was obtained as colorless crystals (MeOH) with molecular composition of $C_{27}H_{44}O_3$, based on HR-TOFMS analysis (Fig. S9). This evaluation elucidated a $[M+H]^+$ ion peak at *m/z* 417.3311 (calcd. for $C_{27}H_{45}O_3$, *m/z* 417.3316), hence six degrees of unsaturation is required. Furthermore, the IR spectrum and NMR data observed in Table 1, Fig. S10 and Fig. S11 were highly similar to **1**. However, the difference was identified in the absence of ketone and acetyl groups, and also the appearance of a newly oxygenated proton [δ_H 4.42 (1H, t, J = 3.2 Hz), δ_C 75.3] and methylene protons [δ_H 1.39 (1H, m), 1.56 (1H, m), δ_C 34.7]. These observations suggest **2** to be de-acetyl and 3-hydroxyl derivative of **1**, which is further supported by the HMBC correlation (Fig. 2c and Fig. S14) from δ_H 4.42 (H-3) to δ_C 34.8 (C-1), 33.7 (C-2) and 37.3 (C-4). The α-orientation of the hydroxyl group at C-3 was determined by the small coupling constant value of H-3 (δ_H 4.42, t, J = 3.2 Hz) and NOESY correlation (Fig. 2b and Fig. S16) between H-3 and CH_3-19. Hence, **2** was determined to be an undescribed dammarane-type triterpenoid, and consequently named pentandrucine B.

Compound **3** was isolated as colorless crystals (MeOH), with molecular formula determined as $C_{32}H_{54}O_5$. This estimation was based on the positive ion peaks at *m/z* 520.7298 $[M+H]^+$ (calcd. for $C_{32}H_{55}O_5$, *m/z* 520.7290) observed in the HR-TOFMS spectrum (Fig. S17). In addition, ^{13}C NMR analyses (Fig. S19) show that six degrees of unsaturation is required, while, the IR absorption bands at 3545, 2971, 1765 and 1085 cm^{-1} imply the presence of hydroxyl, aliphatic, carbonyl ester and ether functionalities. The ^{1}H NMR spectrum data in Table 1 and Fig. S18 show nine tertiary methyls at δ_H 0.82 (CH_3-29), 0.84 (CH_3-19), 0.87 (CH_3-30), 0.92 (CH_3-28), 0.95 (CH_3-18), 1.09 (CH_3-27), 1.13 (CH_3-21), 1.17 (CH_3-26) and 1.95 (CH_3-2′). Also, three oxygenated methines were observed at δ_H 4.33 (1H, t, J = 3.0 Hz), 5.23 (1H, br.s) and 3.62 (1H, dd, J = 4.8 and 10.2 Hz). Meanwhile, the ^{13}C NMR data (Table 1 and Fig. S19) and DEPT spectrum (Fig. S20) displayed 32 carbon resonances, with a tendency to be assigned as nine tertiary methyls (including an acetyl), nine sp^3 methylenes, seven methynes (including three oxygenated sp^3), six quaternary carbons (including two oxygenated types), and one ester carbonyl carbon at δ_C 170.2. These functionalities account for one out of the six degrees of unsaturation, hence five rings are required in **3**. In addition, a combination of the data above with biogenetic considerations suggests compound **3** to be a dammarane-type triterpenoid, characterized by an acetyl and also hydroxyl groups (Phongmaykin et al., 2008). The planar structure was deduced using ^{1}H–^{1}H–COSY and HMBC spectrum analysis (Fig. 3a, Fig. S22 and Fig. S23), and the carbon framework observed was similar to cabraleadiol (Phongmaykin et al., 2008). Furthermore, the only acetyl group present was located at C-7, based on the HMBC correlations of H-7 (δ_H 5.23) to C-5 (δ_C 49.6), C-9 (δ_C 50.7) and C-1′ (δ_C 170.2) and CH_3-2′ (δ_H 1.95) to C-1′ (δ_C 170.2). Proton at H-17 (δ_H 1.83) to C-20 (δ_C 86.7), C-21 (δ_C 27.3) and C-22 (δ_C 35.3), while proton CH_3-21 (δ_H 1.13) to C-17 (δ_C 49.8) and C-22 (δ_C 35.3) is the furan ring correlation. Also,

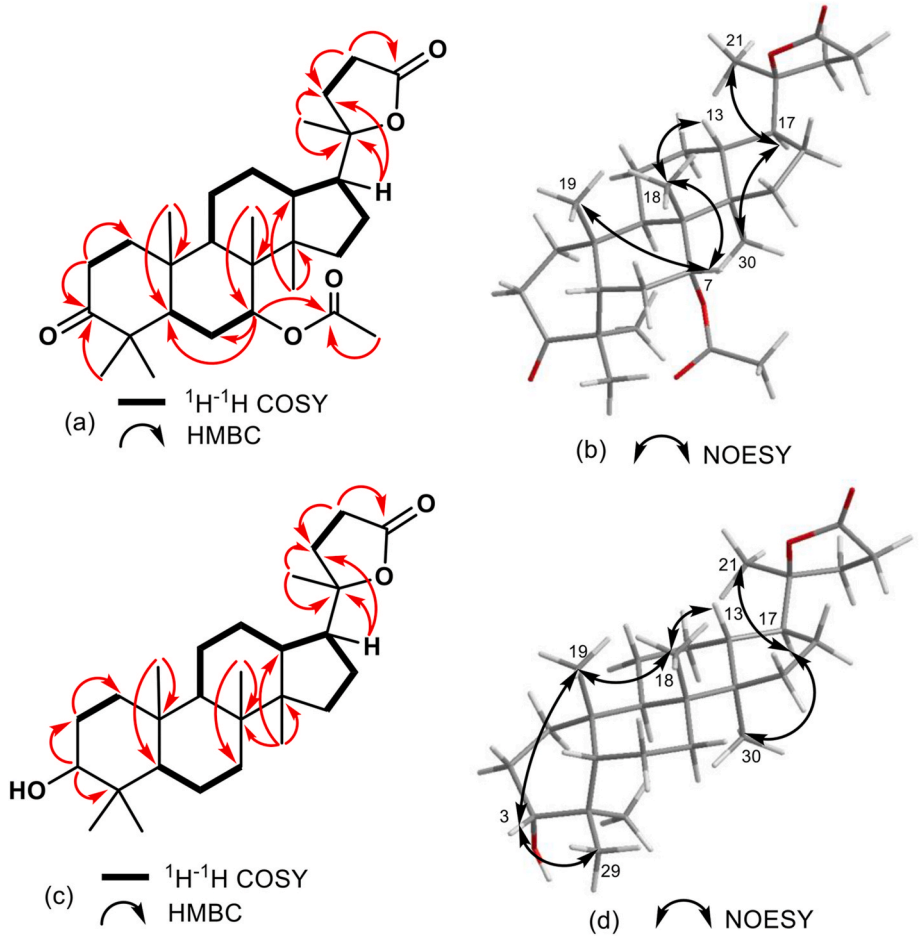

Fig. 2. (a) Selected COSY and HMBC correlations of **1** (b) Selected NOESY correlations of **1** (c) Selected COSY and HMBC correlations of **2** and (d) Selected NOESY correlations of **2**.

the correlation from isopropyl alcohol at H-24 (δ_H 3.62) to C-25 (δ_C 70.3), C-26 (δ_C 27.9) and C-27 (δ_C 24.1), otherwise CH_3-26 (δ_H 1.17) and CH_3-27 (δ_H 1.09) to C-24 (δ_C 86.3).

The relative configuration of **3** was determined with NOESY correlations (Fig. 3b and Fig. S24) and also through NMR data comparison with cabraleadiol (Phongmaykin et al., 2008). The hydroxyl group at C-3 was fixed as α-orientation by the NOESY correlations of H-3/CH_3-19/CH_3-18 and by the small coupling constant value of H-3 (δ_H 4.33, t, J = 3.0 Hz). Furthermore, correlations between H-7/CH_3-18/CH_3-19 and coupling constant value of H-7 (δ_H 5.23, br.s), confirms the α-orientation of acetyl at C-7. The typically observed NOESY correlations of H-5α/H-9α, CH_3-30 (14α-CH_3)/H-17α, H-9α/CH_3-30, CH_3-18/H-13β, revealed that **3** had the same orientation as other reported dammarane-type triterpenoids (Yan et al., 2014; Bai et al., 2018). Based on these descriptions, the structure of **3** was elucidated as 7α-acetyl of cabraleadiol and named pentandrucine C.

Compound **4** possesses a same molecular formula to **3**, $C_{32}H_{54}O_5$, as determined by HR-TOFMS analysis, with molecular formula determined as $C_{32}H_{54}O_5$. This estimation was based on the positive ion peaks at *m/z* 520.8349 [M+H]+(calcd. $C_{32}H_{55}O_5$ *m/z* 520.8310), observed in the HR-TOFMS spectrum (Fig. S25). The IR spectrum confirmed identical functional groups, while the NMR data in Table 1, Fig. S26 and Fig. S27, showed slight variation at C-7 (δ_C 71.3 for **4** and 75.4 for **3**) and C-3 (δ_C 75.4 for **4** and 71.3 for **3**). Based on the observations, **4** was identified as the probable C-3 and C-7 regioisomer of **3**. Furthermore, HMBC correlations (Fig. 3c and Fig. S30) from oxygenated methyne at δ_H 5.23 to C-1 (δ_C 33.7), C-2 (δ_C 25.4), C-4 (δ_C 37.3) and C-1′ (δ_C 170.0), indicates the attachment of an acetyl group at C-3, while the hydroxyl group located at C-7 was denoted by the correlations from oxygenated methyne at δ_H 3.43 to C-6 (δ_C 18.3) and C-8 (40.7). The α-orientation of the acetyl group at C-3 was assigned by the small coupling constant value of H-3 (δ_H 5.23, t, J = 3.0 Hz) and NOESY correlations (Fig. 3d and Fig. S32) of H-3/CH_3-29 and CH_3-19. Meanwhile, the α-orientation of hydroxyl at C-7 was determined from NOESY correlations of H-7/CH_3-19/CH_3-18 and from the coupling constant value of H-7 (δ_H 3.43, t, J = 2.3 Hz), revealing **4** as an undescribed dammarane-type triterpenoid and named pentandrucine D.

Compound **5** was obtained as colorless crystals (MeOH), with a characteristic molecular formula of $C_{34}H_{56}O_6$, based on HRTOFMS ion (Fig. S33) at *m/z* 561.2149 $[M+H]^+$ (calcd. for $C_{34}H_{57}O_6$ *m/z* 561.2139), requiring seven degrees of unsaturation. Furthermore, the IR and 1D NMR data (Table 2, Fig. S34 and Fig. S35) suggests analogous features with **3**. However, differences were recorded by the replacement of an oxygenated methyne signal present in **3** by a resonance at δ_H 5.23 (H-3, t, J = 3.0 Hz) and 1.97 (3H, s), and also as δ_C 21.2, 75.4 and 170.0 in spectrum of **5**. This phenomenon indicates **5** as an acetyl analogue of **3**, while HMBC correlations (Fig. 3e and Fig. S38), from H-3 to C-1 (δ_C 33.7), C-1' (δ_C 170.1), C-4 (δ_C 37.3), show the novel attachment of an acetyl group at C-3. The α-orientation of acetyl at C-3 and C-7 were determined from the coupling constant values of H-3 (δ_H 5.23, t, J = 3.0 Hz) and H-7 (δ_H 5.33, br.s) in H-NMR as well as the NOESY spectrum (Fig. 3f and Fig. S40), with correlations of H-3/CH_3-19 and H-7/CH_3-18 and CH_3-19. Hence, compound **5** was elucidated as an undescribed dammarane-type triterpenoid, and consequently named pentandrucine E.

Compound **6** was obtained as colorless crystals (MeOH), with a

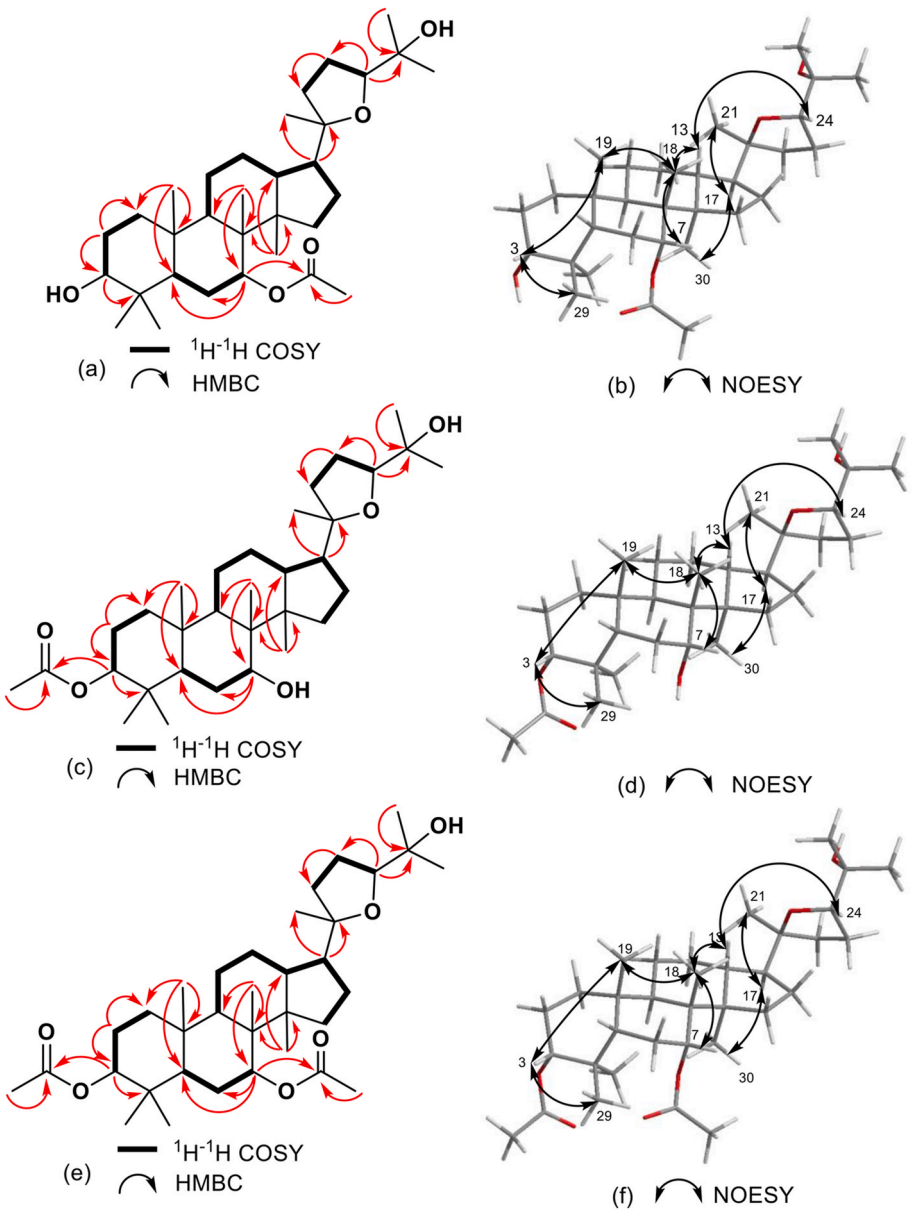

Fig. 3. (a) Selected COSY and HMBC correlations of **3** (b) Selected NOESY correlations of **3** (c) Selected COSY and HMBC correlations of **4** (d) Selected NOESY correlations of **4** (e) Selected COSY and HMBC correlations of **5** and (f) Selected NOESY correlations of **5**.

molecular formula determined as $C_{32}H_{54}O_4$ using HR-TOFMS (Fig. S41) *m/z* 525.2049 $[M+Na]^+$ (calcd. $C_{32}H_{54}NaO_4$ *m/z* 525.2030), indicating six degrees of unsaturation. In addition, IR and NMR data (Table 2, Fig. S42 and Fig. S43) show close similarity to **4**. However, a hydroxyl group absent at C-7 (δ_H 3.43, δ_C 71.3) and methylene signals identified (δ_H 1.13, 1.23, δ_C 34.2), suggests **6** as a 7-dehydroxy derivative of **4**. The HMBC correlations of **6** (Fig. 4a and Fig. S46) between H-3 to C-2 (δ_C 25.4) C-1' (δ_C 170.0) and C-4 (δ_C 37.3), denotes the attachment of an acetyl group at C-3. Furthermore, both comprise of similar relative configuration, based on the NOESY spectrum (Fig. 4b and Fig. S48), with correlations of H-3/CH_3-18 and CH_3-19, and the small coupling constant value of H-3 (δ_H 5.23, t, J = 3.0 Hz), suggesting the acetyl at C-3 as α-oriented. Hence, the structure elucidated was named pentandrucine F.

Compound **7** was obtained as colorless crystals (EtOAc), with a characteristic molecular formula of $C_{30}H_{52}O_4$. This was determined by the combined analyses of HR-TOFMS at *m/z* 477.7431 [M+H]+(calcd. $C_{30}H_{53}O_4$ *m/z* 477.7421) and NMR data (Table 2, Fig. S50 and Fig. S51), which indicated five indices of hydrogen deficiency. The IR and NMR data (Table 2, Fig. S50 and Fig. S51) show close similarity with **3**, differing based on the absence of an acetyl group at C-7 (δ_H 1.95, δ_C 21.2, 170.2) and the presence of oxygenated methyne signals [(δ_H 4.43 (1H, br.s), δ_C 75.1)]. This assessment denotes **7** as a 7-deacetyl derivative of **3**. The HMBC correlations (Fig. 4c and Fig. S54) between H-3/CH_3-28, C-1, C-4 and C-5, as well as H-7/C-9, CH_3-18 and C-5 signified the assignment of two hydroxyl groups at C-3 and C-7, respectively. Meanwhile, the similarity in relative configuration of both compounds was confirmed by NOESY spectrum comparison, where correlations of H-3/CH_3-29/CH_3-19 and H-7/CH_3-19/CH_3-18 (Fig. 4d and Fig. S56) as well as the small coupling constant values of H-3 (δ_H 4.23, t, J = 2.4 Hz) and H-7 (δ_H 4.43, br.s), suggest an α-orientation in the two hydroxyl groups. Hence, the structure of **7** was determined and named pentandrucine G.

Compound **8** was obtained as colorless crystals (MeOH), characterized by the molecular formula $C_{30}H_{50}O_4$. This was determined by the combined analyses of HR-TOFMS (Fig. S57) *m/z* 497.7420 $[M+Na]^+$ (calcd. $C_{30}H_{50}NaO_4$ *m/z* 497.7431) and NMR data (Table 2, Fig. S58 and

Table 2
NMR data for compounds **5–8** (500 MHz for ^{1}H and 125 MHz for ^{13}C in $CDCl_3$).

Position Carbon	5		6		7		8	
	^{13}C-NMR δ_C (mult.)	^{1}H-NMR δ_H [(ΣH, mult., *J*(Hz)]	^{13}C-NMR δ_C (mult.)	^{1}H-NMR δ_H [(ΣH, mult., *J*(Hz)]	^{13}C-NMR δ_C (mult)	^{1}H-NMR δ_H [(ΣH, mult., *J*(Hz)]	^{13}C-NMR δ_C (mult.)	^{1}H-NMR δ_H [(ΣH, mult., *J*(Hz)]
1	33.7 (t)	1.42 (1H, m) 1.84 (1H, m)	33.7 (t)	1.42 (1H, m) 1.87 (1H, m)	33.7 (t)	1.42 (1H, m) 1.86 (1H, m)	33.7 (t)	1.42 (1H, m) 1.83 (1H, m)
2	25.4 (t)	1.55 (1H, m) 2.32 (1H, m)	25.4 (t)	1.55 (1H, m) 2.34 (1H, m)	25.4 (t)	1.55 (1H, m) 2.30 (1H, m)	25.4 (t)	1.55 (1H, m) 2.36 (1H, m)
3	75.4 (d)	5.23 (1H, t, 3.0)	76.3 (d)	5.23 (1H, t, 3.0)	74.1 (d)	4.23 (1H, t, 2.4)	218.4 (s)	–
4	37.3 (s)	–	37.3 (s)	–	37.3 (s)	–	37.3 (s)	–
5	49.6 (d)	1.24 (1H, m)	49.6 (d)	1.24 (1H, m)	49.6 (d)	1.24 (1H, m)	49.6 (d)	1.24 (1H, m)
6	18.3 (t)	1.39 (1H, m) 2.16 (1H, m)	18.3 (t)	1.39 (1H, m) 2.18 (1H, m)	18.3 (t)	1.39 (1H, m) 2.20 (1H, m)	18.3 (t)	1.39 (1H, m) 2.16 (1H, m)
7	76.6 (d)	5.33 (1H, br.s)	34.2 (t)	1.13 (1H, m) 1.23 (1H, m)	75.1 (d)	4.43 (1H, br.s)	71.3 (d)	3.13 (1H, t, 2.3)
8	40.7 (s)	–	40.7 (s)	–	40.7 (s)	–	40.7 (s)	–
9	50.7 (d)	1.44 (1H, m)	50.7 (d)	1.44 (1H, m)	50.7 (d)	1.44 (1H, m)	50.7 (d)	1.44 (1H, m)
10	37.7 (s)	–	37.7 (s)	–	37.7 (s)	–	37.7 (s)	–
11	21.7 (t)	1.53 (1H, m) 1.65 (1H, m)	21.7 (t)	1.53 (1H, m) 1.72 (1H, m)	21.7 (t)	1.53 (1H, m) 1.68 (1H, m)	21.7 (t)	1.53 (1H, m) 1.64 (1H, m)
12	27.1 (t)	1.75 (1H, m) 1.45 (1H, m)	27.1 (t)	1.75 (1H, m) 1.47 (1H, m)	27.1 (t)	1.75 (1H, m) 1.48 (1H, m)	27.1 (t)	1.75 (1H, m) 1.54 (1H, m)
13	42.8 (d)	1.62 (1H, m)	42.8 (d)	1.62 (1H, m)	42.8 (d)	1.62 (1H, m)	42.8 (d)	1.62 (1H, m)
14	50.2 (s)	–	50.2 (s)	–	50.2 (s)	–	50.2 (s)	–
15	31.5 (t)	1.04 (1H, m) 1.82 (1H, m)	31.5 (t)	1.04 (1H, m) 1.83 (1H, m)	31.5 (t)	1.04 (1H, m) 1.80 (1H, m)	31.5 (t)	1.04 (1H, m) 1.78 (1H, m)
16	25.9 (t)	1.51 (1H, m) 2.18 (1H, m)	25.9 (t)	1.51 (1H, m) 2.20 (1H, m)	25.9 (t)	1.51 (1H, m) 2.22 (1H, m)	25.9 (t)	1.51 (1H, m) 1.76 (1H, m)
17	49.8 (d)	1.83 (1H, m)	49.8 (d)	1.83 (1H, m)	49.8 (d)	1.83 (1H, m)	49.8 (d)	1.83 (1H, m)
18	16.2 (q)	0.95 (3H, s)	16.2 (q)	0.95 (3H, s)	16.2 (q)	0.95 (3H, s)	16.2 (q)	0.95 (3H, s)
19	16.6 (q)	0.84 (3H, s)	16.6 (q)	0.84 (3H, s)	16.6 (q)	0.84 (3H, s)	16.6 (q)	0.84 (3H, s)
20	86.7 (s)	–	86.7 (s)	–	86.7 (s)	–	86.7 (s)	–
21	27.3 (q)	1.13 (3H, s)	27.3 (q)	1.13 (3H, s)	27.3 (q)	1.13 (3H, s)	27.3 (q)	1.13 (3H, s)
22	35.3 (t)	1.22 (1H, m) 2.53 (1H, m)	35.3 (t)	1.22 (1H, m) 2.60 (1H, m)	35.3 (t)	1.22 (1H, m) 2.55 (1H, m)	35.3 (t)	1.22 (1H, m) 2.60 (1H, m)
23	26.4 (t)	1.85 (1H, m) 2.64 (1H, m)	26.4 (t)	1.85 (1H, m) 2.62 (1H, m)	26.4 (t)	1.85 (1H, m) 2.64 (1H, m)	26.4 (t)	1.85 (1H, m) 2.74 (1H, m)
24	86.3 (d)	3.62 (1H, dd, 4.8, 10.2)	86.3 (d)	3.62 (1H, dd, 4.8, 10.2)	86.3 (d)	3.62 (1H, dd, 4.8, 10.2)	86.3 (d)	3.62 (1H, dd, 4.8, 10.2)
25	70.3 (s)	–	70.3 (s)	–	70.3 (s)	–	70.3 (s)	–
26	27.9 (q)	1.17 (3H, s)	27.9 (q)	1.17 (3H, s)	27.9 (q)	1.17 (3H, s)	27.9 (q)	1.17 (3H, s)
27	24.1 (q)	1.09 (3H, s)	24.1 (q)	1.09 (3H, s)	24.1 (q)	1.09 (3H, s)	24.1 (q)	1.09 (3H, s)
28	28.4 (q)	0.92 (3H, s)	28.4 (q)	0.92 (3H, s)	28.4 (q)	0.92 (3H, s)	28.4 (q)	0.92 (3H, s)
29	22.2 (q)	0.82 (3H, s)	22.2 (q)	0.82 (3H, s)	22.2 (q)	0.82 (3H, s)	22.2 (q)	0.82 (3H, s)
30	15.6 (q)	0.87 (3H, s)	15.6 (q)	0.87 (3H, s)	15.6 (q)	0.87 (3H, s)	15.6 (q)	0.87 (3H, s)
1′	170.1 (s)		170.0 (s)	–	–	–	–	–
2′	21.2 (q)	1.94 (3H, s)	21.2 (q)	1.97 (3H, s)	–	–	–	–
1′′	170.0 (s)	–						
2′′	21.2 (q)	1.97 (3H, s)						

Fig. S59), showing six degrees of unsaturation is required. The IR and NMR data (Table 2, Fig. S58 and Fig. S59) were closely similar to **7**, except for the disappearance of one oxygenated signal at C-3 [(δ_H 4.23 (1H, t, J = 2.4 Hz), δ_C 74.1)] and the presence of carbonyl signal at δ_C 218.4. This result suggests **8** as a 3-oxo derivative of **7**. In addition, Key HMBC correlations (Fig. 4e and Fig. S27) of H-2/C-3 and CH_3-29/C-3, indicate the attachment of a ketone at C-3. Also, the NOESY spectrum (Fig. 4f and Fig. S62) and small coupling constant value of H-7 (δ_H 3.13, t, J = 2.3 Hz), imply relative similarity between the configurations of both compounds and ocotillone (Aalbersberg and Singh., 1991). Hence, the structure of **8** was determined and named pentandrucine H.

Compound **9** was obtained as colorless crystals (MeOH), with characteristic molecular composition of $C_{27}H_{42}O_4$. This was determined through combined analyses of HR-TOFMS (Fig. S65) *m/z* 431.1471 $[M+H]^+$ (calcd. $C_{27}H_{43}O_4$ *m/z* 431.1402) and NMR data (Table 3, Fig. S66 and Fig. S67), indicating that seven degrees of unsaturation are required. The IR absorption bands at 3518, 1736 and 1085 cm^{-1} imply the presence of hydroxyl, carbonyl and ether groups, while the ^{1}H NMR spectrum (Fig. S66) demonstrates the presence of five tertiary methyl signals at δ_H 0.81 (CH_3-29), 0.87 (CH_3-30), 0.91 (CH_3-28), 0.92 (CH_3-18) and 1.36 (CH_3-21) and also an oxygenated methylene at δ_H [4.39 (1H, d, J = 8.6 Hz), δ_H 3.70 (1H, d, J = 8.6 Hz)]. Furthermore, ^{13}C NMR and DEPT data (Table 3, Fig. S67 and Fig. S68) recognized 27 carbon resonances, attributed to five tertiary methyls, eleven methylenes (including one oxygenated at δ_C 71.4), four methynes, six quaternary carbons (comprising two oxygenated at δ_C 90.3 and 92.1, respectively), and a carbonyl lactone at δ_C 176.9. These functionalities account for one out of seven degrees of unsaturation, hence six additional rings are required. Also, the aforementioned data indicate **9** as a dammarane-type triterpenoid, with lactone and hemi ketal rings, assumed to be formed at C-3 to C-19, based on the HMBC correlations (Fig. 5a, Fig. S70) between H-2 (δ_H 1.46) to C-3 (δ_C 92.1) and CH_2-19 (δ_H 4.39 and 3.70) to C-10 (δ_C 37.7) and C-5 (δ_C 49.9). Proton at H-17 (δ_H 1.23) to C-20 (δ_C 90.3), C-21 (δ_C 25.4) and C-22 (δ_C 31.3), proton CH_3-21 (δ_H 1.36) to C-17 (δ_C 49.5) and C-22 (δ_C 31.3) are the δ-lactone ring correlations. Furthermore, the NMR data showed a close resemblance to amblyone (Harraz et al., 1995), with a slight difference at C-21 (δ_C 25.4 for **9** and δ_C 23.3 for amblyone), indicating **9** as the probable C-21 epimer of amblyone. The signal for C-21 (δ_C 25.4) in **9** was highly similar to 17α-hydroxycabralealactone (δ_C 25.4) (Nagaya et al., 1997), thus indicating the presence of α-orientated CH_3-21. This assessment was supported by the NOESY correlation (Fig. 5b and Fig. S72) between H-17/CH_3-30 and CH_3-21, and the compound structure was defined as an undescribed C-21 epimer of amblyone, and named pentandrucine I.

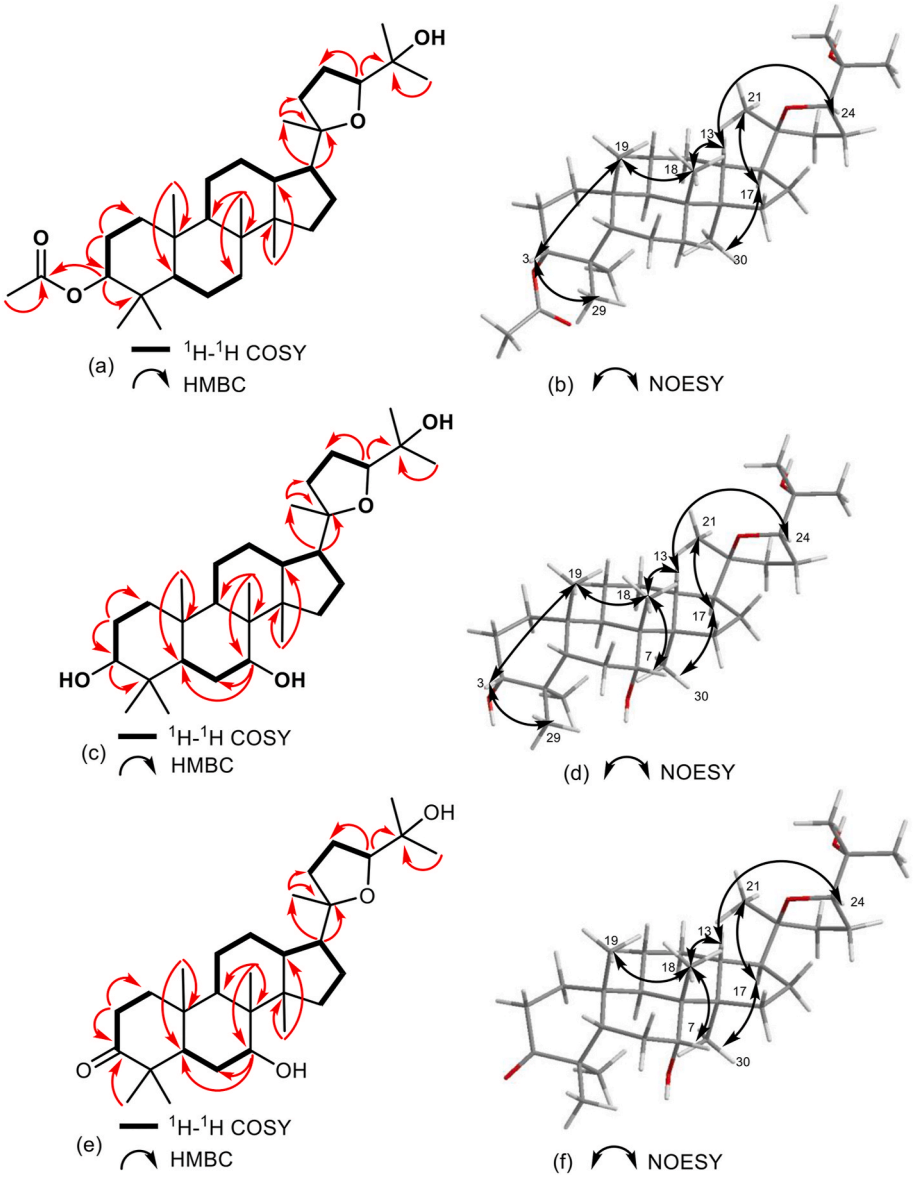

Fig. 4. (a) Selected COSY and HMBC correlations of **6** (b) Selected NOESY correlations of **6** (c) Selected COSY and HMBC correlations of **7** (d) Selected NOESY correlations of **7** (e) Selected COSY and HMBC correlations of **8** and (f) Selected NOESY correlations of **8**.

Compound **10** was obtained as colorless crystals (MeOH), with a suggested molecular formula of $C_{27}H_{42}O_5$. This was determined through the HR-TOFMS spectrum (Fig. S73) *m/z* 447.3012 $[M+H]^+$ (calcd. $C_{27}H_{43}O_5$ *m/z* 447.3029) and NMR data (Table 3, Fig. S74 and Fig. 75), and seven indices of hydrogen deficiency were required. Furthermore, the IR and NMR data was highly similar to **9.** However, differences were observed in the disappearance of methylene signals [δ_H 1.14 (1H, m), 1.23 (1H, m), δ_C 34.7] and the appearance of oxygenated methyne signals [δ_H 4.67 (1H, br.s), δ_C 76.3), suggesting **10** as a 7-hydroxy derivative of **9**. The HMBC correlation (Fig. 5c and Fig. S78), of H-7 (δ_H 4.67) to C-9 (δ_C 50.4), C-6 (δ_C 18.3) and C-5 (δ_C 49.4), indicates the attachment of the novel hydroxyl at C-7. The α-orientation of the hydroxyl group at C-7 was identified from the coupling constant value H-7 (δ_H 4.67, br.s) and NOESY spectrum (Fig. S80) analysis with correlations of H-7/CH_3-18/H-13. Hence, the structure was established and named pentandrucine J.

Compound **11** was isolated as a colorless needles crystal (MeOH), with characteristic a molecular formula of $C_{30}H_{44}O_5$. This was determined through the combined analyses of HR-TOFMS (Fig. S81) *m/z* 485.1872 $[M+H]^+$ (calcd. $C_{30}H_{45}O_5$ *m/z* 485.1852) and NMR data (Table 3, Fig. S82 and Fig. S83), indicating a requirement for eight degrees of unsaturation. The UV spectrum shows maximum absorption at 247 nm (log ε 3.13), indicating the occurrence of an enone group (Shiono et al., 2016), while IR absorption bands at 3417, 3050, 1776 and 1060 cm^{-1} imply the presence of hydroxyl, olefinic, carbonyl and ether functionalities. Furthermore, the ^{1}H NMR spectrum (Table 3 and Fig. S82) demonstrates the presence of seven tertiary methyls [δ_H 1.01 (CH_3-19), 1.06 (CH_3-28), 1.06 (CH_3-29), 1.16 (CH_3-18), 1.16 (CH_3-30), 1.35 (CH_3-26) and 1.44 (CH_3-27)], an olefinic proton at δ_H 5.28 (1H, br. s), two oxygenated methynes [δ_H 4.47 (1H, dd, J = 9.6, 1.8 Hz) and δ_H 3.92 (1H, d, J = 9.6 Hz)] and two olefinic protons [δ_H 7.14 (1H, d, J = 10.2 Hz) and δ_H 5.86 (1H, d, J = 10.2 Hz)] in *cis* configuration. Moreover, the ^{13}C NMR spectrum (Table 3 and Fig. S83) recognized 30 nonequivalent carbon signals, characterized by one carbonyl ketone (δ_C 204.6), a lactone (δ_C 178.6), four sp^2 carbons (δ_C 158.8, 125.7, 157.9 and 119.0), seven methyl signals at (δ_C 16.2, 19.1, 20.0, 21.4, 23.8, 26.9 and 27.1), six sp^3 methylenes, six sp^3 methynes (including two oxygenated carbon at δ_C 78.2 and 74.4) and five quaternary carbons sp^3 (including one oxygenated types at δ_C 72.5), using the classification by DEPT and HMQC experiments (Fig. S84 and Fig. S85). Also, a

Table 3
NMR data for compounds **9–10** (500 MHz for ^{1}H and 125 MHz for ^{13}C in $CDCl_3$) and **11** (600 MHz for ^{1}H and 150 MHz for ^{13}C in $CDCl_3$).

Position Carbon	9		10		11	
	^{13}C-NMR δ_C (mult.)	^{1}H-NMR δ_H [(ΣH, mult., *J* (Hz)]	^{13}C-NMR δ_C (mult.)	^{1}H-NMR δ_H [(ΣH, mult., *J* (Hz)]	^{13}C-NMR δ_C (mult.)	^{1}H-NMR δ_H [(ΣH, mult., *J* (Hz)]
1	35.5 (t)	1.20 (1H, m) 1.50 (1H, m)	35.2 (t)	1.17 (1H. m) 1.50 (1H. m)	158.8 (d)	7.14 (1H, d, 10.2)
2	33.7 (t)	1.46 (1H, dd, 2.3, 9.0) 2.70 (1H, m)	33.7 (t)	1.40 (1H, dd, 2.4, 9.6) 2.74 (1H, m)	125.7 (d)	5.86 (1H, d, 10.2)
3	92.1 (s)	–	92.1 (s)	–	204.6 (s)	–
4	37.3 (s)	–	37.3 (s)	–	44.6 (s)	–
5	49.9 (d)	1.90 (1H, m)	49.4 (d)	1.95 (1H, m)	46.2 (d)	2.20 (1H, m)
6	18.3 (t)	1.36 (1H, m) 2.54 (1H, m)	18.3 (t)	1.37 (1H, m) 2.57 (1H, m)	27.5 (t)	2.25 (1H, m) 2.53 (1H, m)
7	34.7 (d)	1.14 (1H, m) 1.23 (1H, m)	76.3 (d)	4.67 (1H, br. s)	34.8 (t)	1.54 (1H, m) 1.62 (1H, m)
8	40.6 (s)	–	40.6 (s)	–	42.8 (s)	–
9	50.4 (d)	1.48 (1H, dd, 2.6, 13.2)	50.4 (d)	1.41 (1H, dd, 2.4, 13.2)	37.4 (d)	2.19 (1H, m)
10	37.7 (s)	–	37.7 (s)	–	39.7 (s)	–
11	25.4 (t)	1.20 (1H, m) 2.88 (1H, m)	25.4 (t)	1.20 (1H, m) 2.86 (1H, m)	34.1 (t)	1.50 (1H, m) 2.84 (1H, m)
12	21.3 (t)	1.49 (1H, m) 1.91 (1H, m)	21.3 (t)	1.49 (1H, m) 1.91 (1H, m)	38.3 (t)	1.57 (1H, m) 1.90 (1H, m)
13	43.2 (d)	1.53 (1H, m)	43.2 (d)	1.53 (1H, m)	46.8 (s)	–
14	50.3 (s)	–	50.3 (s)	–	157.9 (s)	–
15	31.2 (t)	1.90 (1H, m) 1.10 (1H, m)	31.2 (t)	1.90 (1H, m) 1.10 (1H, m)	119.0 (d)	5.28 (1H, br. s)
16	25.1 (t)	1.52 (1H, m) 1.78 (1H, m)	25.1 (t)	1.52 (1H, m) 1.80 (1H, m)	33.8 (t)	1.17 (1H, m) 1.78 (1H, m)
17	49.5 (d)	1.23 (1H, m)	49.5 (d)	1.23 (1H, m)	58.2 (d)	2.19 (1H, m)
18	15.6 (q)	0.92 (3H, s)	15.6 (q)	0.92 (3H, s)	16.2 (q)	1.16 (3H, s)
19	71.4 (t)	4.39 (1H, d, 8.6) 3.70 (1H, d, 8.6)	71.4 (t)	4.24 (1H, d, 8.9) 3.70 (1H, d, 8.9)	19.1 (q)	1.01 (3H, s)
20	90.3 (s)	–	90.3 (s)	–	44.7 (s)	2.71 (1H, m)
21	25.4 (q)	1.36 (3H, s)	25.4 (q)	1.36 (3H, s)	178.6 (s)	–
22	31.3 (t)	1.49 (1H, m)	31.3 (t)	1.49 (1H, m)	33.1 (t)	1.82 (1H, m)
23	29.3 (t)	2.53 (1H, m) 2.54 (1H, d, 9.9) 2.64 (1H, d, 9.9)	29.3 (t)	2.53 (1H, m) 2.54 (1H, d, 9.9) 2.64 (1H, d, 9.9)	78.2 (d)	2.05 (1H, m) 4.47 (1H, dd, 9.6, 1.8)
24	176.9 (s)	–	176.9 (s)	–	74.4 (d)	3.92 (1H, d, 9.6)
25	–	–	–	–	72.5 (s)	–
26	–	–	–	–	26.9 (q)	1.35 (3H, s)
27	–	–	–	–	23.8 (q)	1.44 (3H, s)
28	28.4 (q)	0.91 (3H, s)	28.4 (q)	0.91 (3H, s)	20.0 (q)	1.06 (3H, s)
29	22.2 (q)	0.81 (3H, s)	22.2 (q)	0.81 (3H, s)	21.4 (q)	1.06 (3H, s)
30	16.4 (q)	0.87 (3H, s)	16.4 (q)	0.87 (3H, s)	27.1 (q)	1.16 (3H, s)

combination of NMR data and literature studies suggest **11** as an analogue of prototiamin A, an apotirucallane-type triterpenoid isolated from the bark of *Entandrophragma congoense* (Happi et al., 2015). However, a major difference is observed with the acetyl group absent [δ_H 1.96 (3H, s), δ_C 21.5 (CH_3), 170.3], and the presence of methylene signals [δ_H 1.62 (1H, m), 1.54 (1H, m), δ_C 34.8 (t)], suggesting **11** to be a de-acetyl derivative of prototiamin A. Furthermore, the olefinic present was located at C-14 and C-15, based on the HMBC correlations (Fig. S86) of CH_3-18 (δ_H 1.16) and CH_3-30 (δ_H 1.16) to C-14 (δ_C 157.9) and H-15 (δ_H 5.28) to C-8 (δ_C 42.8), C-13 (δ_C 46.8) and C-17 (δ_C 58.2). Proton at H-17 (δ_H 2.19) to C-15 (δ_C 119.0), C-21 (δ_C 178.6) and C-22 (δ_C 33.1), proton H-23 (δ_H 4.47) to C-22 (δ_C 33.1) and C-24 (δ_C 74.4) are the lactone ring correlations and the hydroxyl at C-24. Also, all assignments were supported by ^{1}H–^{1}H COSY, HMBC evaluation (Fig. 6c, Fig. S86 and Fig. S87), with NOESY spectrum used to confirm similarity in the relative configuration to prototiamin A, with correlations of H-17/CH_3-30, H-22a and H-24, suggesting an α-orientation of the hydroxyl group at C-24 (Fig. 6d and Fig. S88). Hence, compound **11** was determined to be an undescribed tirucallane-type triterpenoid and named pentandrucine K.

The isolated compounds, **1**–**19**, were evaluated against a MCF-7 breast cancer line using a previously described method (Supratman et al., 2019; Supriatno et al., 2018; Skehan et al., 1990), using Cisplatin as a positive control (Hadisaputri et al., 2012; Chavoshi et al., 2017). Compounds **10–11** and **18–19** proved to be the most active (IC_{50} values of 16.84–20.98 μM), and the strongest cytotoxicity was observed with compound **18,** with an IC_{50} value of 16.84 μM, suggested the presence of lactone ring and diol group in side chain can increase the cytotoxic activity. In addition, **7**–**9** and **13** demonstrated moderate effects (24.33–33.12 μM), while the remaining isolates were weak or inactive (Table 4), indicates that presence of carbonyl and hydroxyl can increase cytotoxic activity, whereas the presence of acetyl groups can decrease the cytotoxic activity.

3. Conclusion

Nineteen triterpenoids were isolated from the bark of *C. pentandrus*, encompassing eleven dammarane-type (**1**–**10** and **12**–**13**), five apotirucallane-type triterpenoids (**11** and **14**–**17**) and two tirucallane-

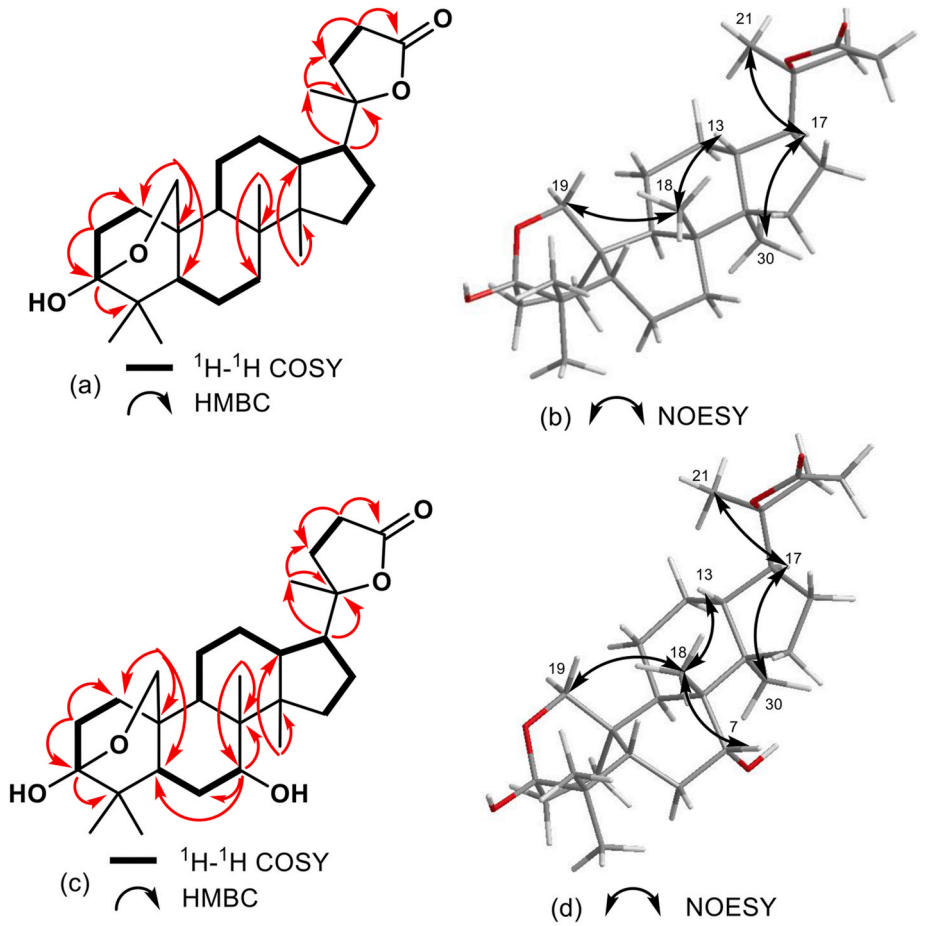

Fig. 5. (a) Selected COSY and HMBC correlations of **9** (b) Selected NOESY correlations of **9** (c) Selected COSY and HMBC correlations of **10** and (d) Selected NOESY correlations of **10**.

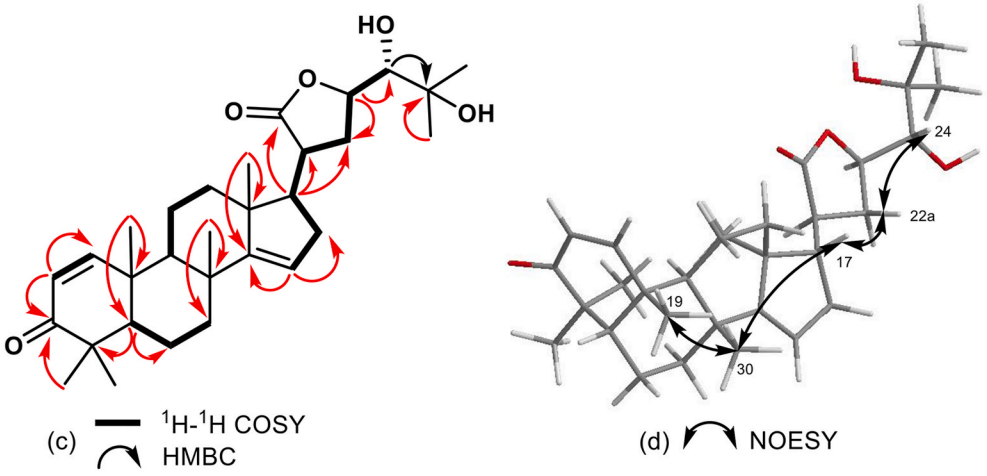

Fig. 6. (a) Selected COSY and HMBC correlations of **11** (b) Selected NOESY correlations of **11**.

type (**18**–**19**). Furthermore, eleven out of these isolates were acknowledged as undescribed compounds, comprising ten dammarane-type (**1**–**10**) and one apotirucallane-type triterpenoid (**11**). The cytotoxic activity was evaluated against MCF-7 breast cancer cell line *in vitro,* and compound **18** (melianodiol) exhibited the strongest activity with an IC_{50} value of 16.84 μM. Carbonyl, hydroxyl and acetyl groups were identified as contributing to the cytotoxic activity.

4. Experimental section

4.1. General experimental procedures

UV spectrum were measured using a TECAN Infinite M200 pro (Mannedorf, Switzerland), while IR involved a SHIMADZU IR Prestige-21 (Kyoto, Japan). The high-resolution time of flight mass spectrometry (HR-TOFMS) data was recorded with Waters Xevo QTOF MS

Table 4
Cytotoxic data for compounds **1–19** against MCF-7 breast cancer cell line.

Compounds	IC_{50} (μM)
Pentandrucine A (**1**)	101.01
Pentandrucine B (**2**)	43.03
Pentandrucine C (**3**)	176.18
Pentandrucine D (**4**)	213.92
Pentandrucine E (**5**)	306.02
Pentandrucine F (**6**)	87.19
Pentandrucine G (**7**)	27.12
Pentandrucine H (**8**)	24.33
Pentandrucine I (**9**)	26.13
Pentandrucine J (**10**)	20.98
Pentandrucine K (**11**)	19.30
Cabrealeolactone (**12**)	61.18
Cabreadiol (**13**)	33.12
Prototiamin A (**14**)	76.08
Neemfruitins A (**15**)	181.12
Desmethyllimocin B (**16**)	98.18
Protoxylocarpin G (**17**)	90.24
Melianodiol (**18**)	16.84
Indicalilacol B (**19**)	20.23
Cisplatin[a]	13.20

[a] Positive control.

(Milford, Massachusetts, USA), and NMR spectrum were evaluated using JEOL ECZ-500 and ECZ-600 (Tokyo, Japan). In addition, the chemical shifts are expressed in ppm, with reference to the $CDCl_3$ (δ_H 7.26/δ_C 77.2) signals. Column chromatography (CC) was performed using silica gel (70–230 mesh and 200–400 mesh) (Merck, Darmstadt, Germany). Thin layer chromatography (TLC) was performed with silica gel 60 F_{254} plates (Merck, 0.25 mm, Darmstadt, Germany). Compounds were visualized under UV light (257 and 364 nm) or by spraying the heated silica gel plates with 10% H_2SO_4 in EtOH.

4.2. Plant material

The stem bark of *C. pentandrus* was collected from Bogor Botanical Garden, Bogor, West Java Province, Indonesia (Latitude: 6° 35′ 30.59'' S; Longitude: 106° 47′ 32.39'' E) in June 2016. The plant was identified by Mr. Ismail, of the Bogoriense Herbarium, Bogor, Indonesia where a voucher specimen (No. Bo-104) is deposited.

4.3. Extraction and isolation

The air-dried stem bark of *C. pentandrus* (1.8 kg) was ground to a powder, extracted with methanol (4 × 4 L, 4 days each) at room temperature, and concentrated using a rotary evaporator, yielding a concentrated extract (340 g). About 300 g of the MeOH extract was suspended in H_2O (600 mL) and successively partitioned with *n*-hexane, EtOAc and *n*-butanol. This was followed by evaporation under reduced pressure, resulting in 10.90, 25.18, and 228.63 g of crude extracts, respectively. In addition, 10.0 g of the *n*-hexane soluble fraction was chromatographed using silica gel CC (200 g, 70–230 mesh), and eluted with *n*-hexane-EtOAc-MeOH (10% stepwise), resulting in eight fractions (Fr. A to Fr. H).

Fr. B (439 mg) was subjected to silica gel CC (50 g, 230–400 mesh) and eluted with *n*-hexane-DCM-EtOAc (5% stepwise) to generate seven fractions (Fr. B1 to Fr. B7). Subsequently, Fr. B3 (230 mg) was purified by crystallization in MeOH to yield **5** (86.2 mg), while Fr. B7 (132.3 mg) was chromatographed using silica gel CC (10 g, 230–400 mesh) with gradient elution of *n*-hexane-DCM-EtOAc (5% stepwise) to produce seven fractions (Fr. B7A to Fr. B7F). Therefore, Fr. B7B (13.2 mg) was separated over silica gel CC (5 g, 230–400 mesh), and eluted with *n*-hexane: DCM (1:1) to yield **13** (2.3 mg). Also, Fr. B7C (43.2 mg) was separated over silica gel CC (6 g, 230–400 mesh), and eluted with *n*-hexane: DCM: EtOAc (5:4.5:0.5) to produce **3** (14.2 mg), while Fr. B7D (20.1 mg) was purified by silica gel CC (5 g, 230–400 mesh), and eluted with *n*-hexane: DCM (6:4) to generate **6** (8.1 mg).

Fraction C (700 mg) was separated over silica gel CC (70 g, 70–230 mesh) with a gradient eluent of *n*-hexane-DCM-EtOAc (5% stepwise) to produce five fractions (Fr. C1 to Fr. C5). Therefore, Fr. C3 (300 mg) was further separated over silica gel CC (30 g, 230–400 mesh), and eluted with *n*-hexane: DCM (4:1) to yield four fractions (Fr. C3A to Fr. C3D). Subsequently, Fr. C3C (110 mg) was purified by silica gel CC (15 g, 230–400 mesh), and eluted with DCM: EtOAc (7.5:2.5) to generate **2** (14.2 mg), while Fr. C3D (14.5 mg) was separated over silica gel CC (5 g, 230–400 mesh), and eluted with $CHCl_3$: EtOAc (6:4) for the isolation of **7** (1.9 mg).

Fraction D (725 mg) was separated over silica gel CC (80 g, 70–230 mesh), using a gradient elution consisting of *n*-hexane-$CHCl_3$-EtOAc (5% stepwise) to generate seven fractions (Fr. D1 - D7). Fr. D4 (141.5 mg) was separated with CC (15 g, 230–400 mesh), and eluted with *n*-hexane: $CHCl_3$: EtOAc (7:1.5:1.5), to yield five fractions (Fr. D4A - D4E), while Fr. D4C (41.2 mg) was purified on CC (5 g, 230–400 mesh), and eluted with DCM: $CHCl_3$: EtOAc (6:1.5:2.5) to produce **1** (11.2 mg), and Fr. D4D (32.5 mg) was separated with CC (5 g, 230–400 mesh), with DCM: EtOAc (7.5:2.5) to obtain **12** (2.1 mg).

Fraction E (820 mg) was chromatographed using silica gel CC (100 g, 70–230 mesh), and eluted with a *n*-hexane-DCM-EtOAc gradient (5% stepwise) to yield eleven fractions (Fr. E1 - E12). Fr. E2 (141.5 mg) was separated over silica gel CC (20 g, 230–400 mesh), and eluted with $CHCl_3$: EtOAc (7.5:2.5), to produce **8** (2.2 mg), while Fr. E3 (342.3 mg) was further separated with silica gel CC (40 g, 70–230 mesh), and eluted with $CHCl_3$: EtOAc (7.5:2.5) to generate four fractions (Fr. E3A to Fr. E3D). Subsequently, Fr. E3C (108.1 mg) was purified by silica gel CC (10 g, 230–400 mesh), and eluted with $CHCl_3$: EtOAc: HOAc (6.5:3:0.5) to obtain **10** (5.3 mg), while Fr. E3CD (28.0 mg) was isolated using silica gel CC (5 g, 230–400 mesh), and eluted with DCM: HOAc: MeOH (8.5:1:0.5) to yield **9** (1.4 mg). In addition, Fr. E5 (213.7 mg) was chromatographed using silica gel CC (40 g, 70–230 mesh), and eluted with $CHCl_3$: EtOAc: MeOH (7.5:2:0.5) to generate five fractions (Fr. E5A - E5E). Fr. E5D (107.7 mg) was separated over silica gel CC (15 g, 230–400 mesh), and eluted with $CHCl_3$: EtOAc: MeOH (7:2:1) to obtain **18** (2.9 mg). Also, Fr. E5E (32.1 mg) was purified by CC (5 g, 230–400 mesh), and eluted with DCM: HOAc: MeOH (6.5:2:1.5) to produce **4** (6.4 mg).

Fraction F (623.9 mg) was chromatographed using silica gel CC (70 g, 70–230 mesh), and eluted with a DCM-EtOAc gradient solvent system (2.5% stepwise) to obtain seven fractions (Fr. F1 – F7). Therefore, Fr. F3 (312.1 mg) was isolated by CC on silica gel (40 g, 230–400 mesh), and eluted with DCM: HOAc: MeOH (6.5:2:1.5), to generate **19** (1.3 mg), while Fr. F3D (100 mg) was separated over CC on silica gel (25 g, 230–400 mesh), and eluted with DCM: HOAc: MeOH (6:2:2), to yield **11** (3.2 mg) and **14** (5.4 mg).

Fraction G (712.2 mg) was chromatographed using silica gel CC (80 g, 70–230 mesh) with an elution gradient of DCM-EtOAc (5% stepwise), to produce six fractions (Fr.G1 - G6). Therefore, Fr. G2 (300 mg) was separated by CC on silica gel (40 g, 70–230 mesh), and eluted with $CHCl_3$: EtOAc: HOAc (5.5:4:0.5) to generate **15** (2.8 mg), while Fr. G3 (101.3 mg) was purified using CC on silica gel (10 g, 230–400 mesh), and eluted with $CHCl_3$: EtOAc: HOAc (5:4.5:0.5) to obtain **17** (2.1 mg). Fr. G4 (42.1 mg) was isolated using CC on silica gel (5 g, 230–400 mesh), and eluted with DCM: HOAc: MeOH (6.5:2:1.5) to yield **16** (1.4 mg).

4.3.1. Pentandrucine A (1)

Colorless needle crystals (MeOH); mp 185–187 °C; $[\alpha]^{25}_D$ + 52 (*c* 0.1, MeOH); IR (KBr) ν_{max} 2964, 2923, 1702, 1687, 1450 and 1085 cm^{-1}; ^1H and ^{13}C-NMR data see Table 1; HR-TOFMS *m/z* 473.3271 [M+H]+(calcd. $C_{29}H_{45}O_5$ *m/z* 473.3241).

4.3.2. Pentandrucine B (2)

Colorless crystal (MeOH); mp 190–192 °C; $[\alpha]^{25}_D$ + 43° (*c* 0.12,

MeOH); IR (KBr) ν_{max} 3396, 2964, 2923, 1702, 1410 and 1085 cm^{-1}; ^{1}H and ^{13}C-NMR, see Table 1; HR-TOFMS *m/z* 417.3311 [M+H]+(calcd. $C_{27}H_{45}O_3$ *m/z* 417.3316).

4.3.3. Pentandrucine C (3)

Colorless crystals (MeOH); mp 178–180 °C; $[\alpha]^{25}_{D}$ + 49° (*c* 0.1, MeOH); IR (KBr) ν_{max} 3545, 2971, 1765, 1613, 1400 and 1085 cm^{-1}; ^{1}H and ^{13}C-NMR, see Table 1; HR-TOFMS *m/z* 520.7299 [M+H]+(calcd. $C_{32}H_{55}O_5$ *m/z* 520.7290).

4.3.4. Pentandrucine D (4)

Colorless needle crystals (MeOH); mp 198–200 °C; $[\alpha]^{25}_{D}$ + 48° (*c* 0.1, MeOH); IR (KBr) ν_{max} 3546, 2971, 1764, 1613, 1400 and 1085 cm^{-1}; ^{1}H and ^{13}C-NMR, see Table 1; HR-TOFMS *m/z* 520.8349 [M+H]+ (calcd. $C_{32}H_{55}O_5$ *m/z* 520.8310).

4.3.5. Pentandrucine E (5)

Colorless crystal (MeOH); mp 167–169 °C; $[\alpha]^{25}_{D}$ + 49° (*c* 0.11, MeOH); IR (KBr) ν_{max} 3096, 2968, 1765, 1613, 1450 and 1085 cm^{-1}; ^{1}H and ^{13}C-NMR, see Table 2; HR-TOFMS *m/z* 561.2149 [M+H]+(calcd. $C_{34}H_{57}O_6$ *m/z* 561.2139).

4.3.6. Pentandrucine F (6)

Colorless crystals (MeOH); mp 171–174 °C; $[\alpha]^{25}_{D}$ + 56° (*c* 0.1, MeOH); IR (KBr) ν_{max} 3016, 2971, 1764, 1613, 1400 and 1085 cm^{-1}; ^{1}H and ^{13}C-NMR ($CDCl_3$, 125 MHz), see Table 2; HR-TOFMS *m/z* 525.2049 $[M+Na]^+$ (calcd. $C_{32}H_{54}NaO_4$ *m/z* 525.2030).

4.3.7. Pentandrucine G (7)

Colorless crystals (EtOAc); mp 153–154 °C; $[\alpha]^{25}_{D}$ −18° (*c* 0.1, MeOH); IR (KBr) ν_{max} 3540, 2971, 1613, 1400, 1383 and 1085 cm^{-1}; ^{1}H and ^{13}C-NMR, see Table 2; HR-TOFMS *m/z* 477.7432 [M+H]+(calcd. $C_{30}H_{53}O_4$ *m/z* 477.7421).

4.3.8. Pentandrucine H (8)

Colorless crystals (MeOH); mp 120–123 °C; $[\alpha]^{25}_{D}$ +36° (*c* 0.03, MeOH); IR (KBr) ν_{max} 3546, 2971, 2921, 2851, 1776, 1401 and 1085 cm^{-1}; ^{1}H and ^{13}C-NMR, see Table 2; HR-TOFMS *m/z* 497.7420 $[M+Na]^+$ (calcd. $C_{30}H_{50}NaO_4$ *m/z* 497.7431).

4.3.9. Pentandrucine I (9)

Colorless crystals (MeOH); mp 141–144 °C; $[\alpha]^{25}_{D}$ +15° (*c* 0.12, $CHCl_3$); IR (KBr) ν_{max} 3518, 3071, 2988, 1736, 1421, 1268, 1085 and 895 cm^{-1}; ^{1}H and ^{13}C-NMR, see Table 3; HR-TOFMS *m/z* 431.1471 $[M+H]^+$ (calcd. $C_{27}H_{43}O_4$ *m/z* 431.1402).

4.3.10. Pentandrucine J (10)

Colorless crystals (MeOH); mp 165–166 °C; $[\alpha]^{25}_{D}$ +18° (*c* 0.03, $CHCl_3$); IR (KBr) ν_{max} 3513, 2998, 1736, 1705, 1430, 1085 and 895 cm^{-1}; ^{1}H and ^{13}C-NMR, see Table 3; HR-TOFMS *m/z* 447.3012 $[M+H]^+$ (calcd. $C_{27}H_{43}O_5$ *m/z* 447.3029).

4.3.11. Pentandrucine K (11)

Colorless needles crystals (MeOH); mp 169–171 °C; $[\alpha]^{25}_{D}$ - 50° (*c* 0.11, $CHCl_3$); UV (MeOH) λ_{max} 247 nm (log ε 3.13); IR (KBr) ν_{max} 3417, 3050, 2974, 2311, 1765, 1665, 1365 and 1085 cm^{-1}; ^{1}H-NMR ($CDCl_3$, 600 MHz), ^{13}C-NMR ($CDCl_3$, 150 MHz), see Table 3; HR-TOFMS *m/z* 485.1872 $[M+H]^+$ (calcd. $C_{30}H_{45}O_5$ *m/z* 485.1852).

4.4. Bioassays for cytotoxic activity

The MCF-7 cells were seeded into 96-well plates with an initial density of approximately 3×10^4 cells cm^{-3}. These were subsequently incubated to facilitate attachment and growth, after the addition of varied sample concentrations. The respective compounds were first dissolved in DMSO, followed by the preparation of six desirable strengths with PBS (phosphoric buffer solution, pH = 7.30–7.65). Furthermore, the control wells received only DMSO, and the assay was terminated after a 48 h incubation period by adding MTT reagent [3-(4,5-dimethylthiazol-2-yl)-2,5-diphenyl tetrazolium bromide; also known as thiazol blue]. Subsequently, another round of incubation was conducted for 4 h, followed by the addition of MTT-stop solution containing SDS (sodium dodecyl sulphate), and the experiment was further incubated for another 24 h. The optical density was read using a micro plate reader at 550 nm, and the IC_{50} values of the percentage live cells recorded from the plotted graph were compared between the control (%), comprising only PBS and DMSO, and samples with the tested compound concentrations (μM). Moreover, IC_{50} value is determined as the concentration required for 50% growth inhibition, and each assay as well as analysis was determined in triplicate and averaged.

Declaration of competing interest

The authors declare that they have no known competing financial interests or personal relationships that could have appeared to influence the work reported in this paper.

Acknowledgements

This research was financially supported by the Directorate of Resources, Directorate General of Higher Education, Ministry of Education and Culture, Indonesia (World Class Professor Grant, No: 101.7/E4.3/KU/2020 by Desi Harneti) and Academic Leadership Grant from Universitas Padjadjaran, Indonesia (No: 1427/UN63.1/LT/2020 by Unang Supratman).

Appendix A. Supplementary data

Supplementary data to this article can be found online at https://doi.org/10.1016/j.phytochem.2021.112759.

References

Aalbersberg, W., Singh, Y., 1991. Dammarane Triterpenoids from *Dysoxylum Richii* Phytochemistry 30 (3), 921–926. https://doi.org/10.1016/0031-9422(91)85280-D.

Ahmad, V.U., Alvi, K.A., 1987. Deacetoxybrachycarpone, A trinortriterpenoid from *Cleome brachycarpa*. Phytochemistry 26 (1), 315–316. https://doi.org/10.1016/s0031-9422(00)81537-x.

Awang, K., Lim, C.S., Mohamad, K., Hiroshi, M., Hirasawa, Y., Takeya, K., Thoison, O., Hadi, A.H.A., 2007. Erythrocarpines A-E, new cytotoxic triterpens from *Chisocheton erythrocarpus*. Bioorg. Med. Chem. 15, 5997–6002. https://doi.org/10.1016/j.bmc.2007.05.049.

Bai, W., Yang, H.Y., Jiao, X.Z., Feng, K.N., Chen, J.J., Gao, K., 2018. Structurally diverse highly oxygenated triterpenoids from the roots of *Ailanthus altissima* and their cytotoxicity. J. Nat. Prod. 81, 1777–1785. https://doi.org/10.1021/acs.jnatprod.8b00208.

Bordoloi, M., Saikia, B., Mathur, R.K., Goswami, B.N., 1993. A meliacin from *Chisocheton panniculatus*. Phytochemistry 34, 583–584. https://doi.org/10.1016/0031-9422(93)80054-V.

Brahmachari, G., 2004. Neem–an omnipotent plant: a retrospection. Chembiochem 5, 408–421. https://doi.org/10.1002/cbic.200300749.

Cascon, S.C., Brown, K.S.J., 1972. Biogenetically significant triterpenes in a species of Meliaceae: *Cabralea polytricha*. A. Juss. Tetrahedron 28 (2), 315–323. https://doi.org/10.1016/0040-4020(72)80138-8.

Chavoshi, H., Vahedian, V., Saghaei, S., Pirouzpanah, M.B., Raeisi, M., Samadi, N., 2017. Adjuvant therapy with silibinin improves the efficacy of paclitaxel and cisplatin in MCF-7 breast cancer cells. Asian Pac. J. Cancer Prev. APJCP 18 (8), 2243–2247. https://doi.org/10.22034/APJCP.2017.18.8.2243.

Chianese, G., Yerbanga, S.R., Lucantoni, L., Habluetzel, A., Basilico, N., Taramelli, D., Fattorusso, E., Scafati, O.T., 2010. Antiplasmodial triterpenoids from the fruits of neem, *Azadirachta indica*. J. Nat. Prod. 73, 1448–1452. https://doi.org/10.1021/np100325q.

Crabbe, P., Ourisson, G., Takahashi, T., 1958. Le Dipterocarpol-I: preparation de la 8,14-dimethyl 18-nor-testosterone. Tetrahedron 3, 279–302. https://doi.org/10.1016/0040-4020(58)80024-1.

Gupta, A.S., Dev, S., 1971. Higher isoprenoids—I, triterpenoids from the oleoresin of *Dipterocarpus pilosus*: hollongdione and dipterocarpolic acid. Tetrahedron 27 (4), 823–834. https://doi.org/10.1016/S0040-4020(01)92478-0.

Hadisaputri, Y.E., Pharm, D., Miyazaki, T., Suzuki, S., Yokobori, T., Kobayashi, T., Tanaka, N., Inose, T., Sohda, M., Kuwano, H., 2012. *TNFAIP8* overexpression:

clinical relevance to esophageal squamous cell carcinoma. Ann. Surg Oncol. 19, S589–S596. https://doi.org/10.1245/s10434-011-2097-1.
Happi, G.M., Kouam, S.F., Talontsi, F.M., Lamshöft, M., Zühlke, S., Bauer, J.O., Strohmann, C., Spiteller, M., 2015. Antiplasmodial and cytotoxic triterpenoids from the bark of the Cameroonian medicinal plant *Entandrophragma congoense*. J. Nat. Prod. 78, 604–614. https://doi.org/10.1021/np5004164.
Harraz, F.M., Ulubelen, A., Oksuz, S., Tan, M., 1995. Dammarane triterpenes from *Cleome amblyyocarpa*. Phytochemistry 39 (1), 175–178. https://doi.org/10.1016/0031-9422(94)00848-N.
Huang, S.S., Jian, K.L., Li, R.J., Kong, L.Y., Yang, M.H., 2016. Phytosteroids and triterpenoids with potent cytotoxicities from the leaves of *Chisocheton cumingianus*. RSC Adv. 6, 6320–6328. https://doi.org/10.1039/c5ra23626f.
Joycharat, N., Plodpai, P., Panthong, K., Yingyongnarongkul, B., Voravuthikuncai, S.P., 2010. Terpenoid constituents and antifungal activity of *Aglaia forbesii* seed against phytopathogens. Can. J. Chem. 88, 937–944. https://doi.org/10.1139/V10-085.
Katja, D.G., Farabi, K., Nurlelasari, Harneti, D., Mayanti, T., Supratman, U., Awang, K., Hayashi, H., 2017. Cytototoxic constituents from the bark of *Chisocheton cumingianus* (Meliaceae). J. Asian Nat. Prod. Res. 6, 1–5. https://doi.org/10.1080/10286020.2016.1196671.
Kumar, C.S.S.R., Srinivas, M., Yakkundi, S., 1996. Limonoids from the seeds of *Azadirachta indica*. Phytochemistry 43 (2), 451–455. https://doi.org/10.1016/0031-9422(96)00226-9.
Kurimoto, S., Takaishi, Y., Ahmed, F.A., Kashiwada, Y., 2014. Triterpenoids from the fruits of *Azadirachta indica* (Meliaceae). Fitoterapia 92, 200–205. https://doi.org/10.1016/j.fitote.2013.11.004.
Maneerat, W., Laphookhieo, S., Koysomboon, S., Chantrapromma, K., 2008. Antimalarial, antimycobacterial and cytotoxic limonoids from *Chisocheton siamensis*. Phytomedicine 15, 1130–1134. https://doi.org/10.1016/j.phymed.2008.05.004.
Mohamad, K., Hirasawa, Y., Litaudon, M., Awang, K., Hamid, A., Hadi, A., Takeya, K., Ekasari, W., Widyawaruyanti, A., Zaini, N.C., 2009. Ceramicines B–D, new antiplasmodial triterpens from *Chisocheton ceramicus*. Bioorg. Med. Chem. 17, 727–730. https://doi.org/10.1016/j.bmc.2008.11.048, 1115−1119.
Nagaya, H., Tobita, Y., Nagae, T., Itokawa, H., Takeya, K., Halim, A.F., Halim, A.O.B., 1997. Cytotoxic triterpenes from *Cleome africana*. Phytochemistry 44 (6), 1115–1119. https://doi.org/10.1016/S0031-9422(96)00681-4.
Nagoor, N.H., Muttiah, N.S.J., Lim, C.S., In, L.L.A., Mohammad, K., Awang, K., 2011. Regulation of apoptotic effects by erythrocarpine e, a cytotoxic limonoid from *Chisocheton erythrocarpus* in HSC-4 human oral Cancer cells. PloS One 6 (8), 1–7. https://doi.org/10.1371/journal.pone.0023661.
Nurlelasari, Katja, D.G., Harneti, D., Wardayo, M.M., Supratman, U., Awang, K., 2017. Triterpens from the seeds of *Chisocheton macrophyllus*. Chem. Nat. Compd. 53, 83–87. https://doi.org/10.1007/s10600-017-1916-4.
Phongmaykin, J., Kumamoto, T., Ishikawa, T., Suttisri, R., Saifah, E., 2008. A new sesquiterpene and other terpenoid constituents of *Chisocheton penduliflorus*. Arch Pharm. Res. (Seoul) 31 (1), 21–27. https://doi.org/10.1007/s12272-008-1115-8.
Puripattanavong, J., Weber, S., Brecht, V., Frahm, A.W., 2000. Phytochemical investigation of *Aglaia andamanica*. Planta Med. 66, 740–745. https://doi.org/10.1055/s-2000-9901.
Shilpi, J.A., Saha, S., Chong, S.L., Nahar, L., Sarker, S.D., Awang, K., 2016. Advances in chemistry and bioactivity of the genus *Chisocheton* BLUME. Chem. Biodivers. 13, 483–503. https://doi.org/10.1002/cbdv.201400373.
Shiono, Y., Miyazani, N., Murayama, T., Koseki, T., Harizon, Katja, D.G., Supratman, U., Nakata, J., Kakihara, Y., Saeki, M., Yoshida, J., Uesugi, S., Kimura, K., 2016. GSK-3β inhibitory activities of novel dichloresorcinol derivatives from *Cosmospora vilior* isolated from a mangrove plant. Phytochem. Lett. 18, 122–127. https://doi.org/10.1016/j.phytol.2016.09.007.
Skehan, P., Storeng, R., Scudiero, D., Monks, A., McMahon, J., Vistica, D., Warren, J.T., Bokesch, H., Kenney, S., Boyd, R.M., 1990. New colorimetric cytotoxicity assay for anticancer-drug screening. J. Natl. Cancer Inst. 82, 1107–1112. https://doi.org/10.1093/jnci/82.13.1107.
Supratman, U., Naibaho, W., Salam, S., Maharani, R., Hidayat, A.T., Harneti, D., Nurlelasari, Shiono, Y., 2019. Cytotoxic triterpenoids from the bark of *Chisocheton patens* blume (Meliaceae). Phytochem. Lett. 30, 81–87. https://doi.org/10.1016/j.phytol.2019.01.034.
Supratman, U., Salam, S., Naibaho, W., Fajar, M., Nurlelasari, Katja, D.G., Harneti, D., Maharani, R., Hidayat, A.T., Lesmana, R., Nafiah, M.A., Shiono, Y., 2020. New cytotoxic limonoids from the stem bark of *Chisocheton pentandrus* (Blanco) Merr. Phytochem. Lett. 35, 63–67. https://doi.org/10.1016/j.phytol.2019.11.002.
Supriatno, Nurlelasari, Herlina, T., Harneti, D., Maharani, R., Hidayat, A.T., Mayanti, T., Supratman, U., Azmi, M.N., Shiono, Y., 2018. A new limonoid from stem bark of *Chisocheton pentandrus* (Meliaceae). Nat. Prod. Res. 32 (21), 2610–2616.
Wong, C.P., Shimada, M., Nagakura, Y., Nugroho, A.E., Hirasawa, Y., Taneda, T., Awang, K., Hadi, A.H.A., Mohamad, K., Shiro, M., Mprita, H., 2011. Ceramicines E-I, new triterpens from *Chisocheton ceramicus*. Chem. Pharm. Bull. 59, 407–411. https://doi.org/10.1248/cpb.59.407.
Yamashita, H., Masuda, K., Kobayashi, T., Ageta, H., Shiojima, K., 1998. Dammarane triterpenoids from rhizomes of *Pyrrosia lingua*. Phytochemistry 49 (8), 2461–2466. https://doi.org/10.1016/s0031-9422(98)00303-3.
Yan, H.J., Wang, J.S., Kong, L.Y., 2014. Cytotoxic dammarane-type triterpenoids from the stem bark of *Dysoxylum binecteriferum*. J. Nat. Prod. 77, 234–242. https://doi.org/10.1021/np400700g.
Yang, M.H., Wang, J.S., Luo, J.G., Wang, X.B., Kong, L.Y., 2009. Tetranortriterpenoids from *Chisocheton paniculatus*. J. Nat. Prod. 72 https://doi.org/10.1021/np900485t, 2014–2018.
Yang, M.H., Wang, J.S., Luo, J.G., Wang, X.B., Kong, L.Y., 2011. Chisopanins A–K, 11 new protolimonoids from *Chisocheton paniculatus* and their anti-inflammatory activities. Bioorg. Med. Chem. 19, 1409–1417. https://doi.org/10.1016/j.bmc.2011.01.007.